

Experimental study of negative differential conductivity in GaAs:Cr

R. M. Rubinger,* A. G. de Oliveira, J. C. Bezerra, G. M. Ribeiro, W. N. Rodrigues, and M. V. B. Moreira
*Departamento de Física, Instituto de Ciências Exatas, Universidade Federal de Minas Gerais, Caixa Postal 702,
 30123-970, Belo Horizonte, Brazil*

(Received 14 September 1999; revised manuscript received 18 February 2000)

We have studied the temperature and illumination dependencies of the current versus voltage characteristics $I(V)$ of a Cr-doped GaAs sample. An S-shaped negative differential conductivity with a threshold at around 1 kV cm^{-1} was associated with a trap with activation energy of 90 meV. The low-conductivity state in $I(V)$ characteristics is strongly influenced by illumination and temperature. We also present evidence that the electrical conduction above the threshold electric field occurs by a mechanism that involves free electrons despite the fact that the low-conductivity state is p type. This supports the assumption that the 90 meV trap is a donor.

INTRODUCTION

The study of instabilities in semiconductors has been a field of intense interest during recent decades, and most of the instabilities display spatiotemporal patterns. The presence of the negative differential conductivity (NDC) effect is usually associated with instabilities of a homogeneous steady state produced by spatial fluctuations in the electric field or in the carrier density. A large variety of semiconductor devices like the Gunn diode¹ and the Impatt diode² take advantage of the NDC effect. The NDC effect is divided into two basic classes, namely, SNDC and NNDC, depending upon whether the $\mathbf{j}(\mathbf{E})$ characteristic resembles the letter S or N. Usually, the SNDC in the $\mathbf{j}(\mathbf{E})$ characteristics presents a low-conductivity state (LCS) followed by a high-conductivity state (HCS) that arises for electric fields higher than a threshold value. Despite the great progress in the study of the NDC effect in recent years, there is not a complete model available to describe all the experimental observations.

Nonintentionally doped GaAs crystals grown by the liquid-encapsulated Czochralski (LEC) technique are usually n type due to Si and S shallow donor impurities with concentrations at around 10^{15} – 10^{16} cm^{-3} , in excess of compensating shallow acceptor impurities. Historically, chromium has been one of the few deep-trap impurities used as a deliberate dopant of III-V compounds in order to produce semi-insulating (SI) materials. The role of Cr atoms is to compensate the common shallow donors and thus the Fermi level is pinned around the mid-gap.^{3,4} This conventional view of the compensation process introduced by Cr is, however, too simple. Indeed, several authors⁵ have concluded that the $EL2$ center may also play an important role in Cr-doped samples. Depending on the effective carrier density ($N_D - N_A$), one of the two deep centers acts as the main deep trap. Another relevant aspect of the electrical characterization of trap-dominated semiconductors is that their characteristics are strongly influenced by so-called near-contact effects.⁶

The Cr-doped (at about 10^{16} cm^{-3}) GaAs samples used in the present work were obtained from a commercial wafer grown by the LEC technique in silica crucibles. The deep level due to the internal transition $\text{Cr}^{3+/2+}$ lies about the

middle of the gap and it is usually considered to be responsible for the SI characteristics of the samples. Impurity breakdown⁷ due to impact ionization of deep traps occurs at electric fields of a few kV cm^{-1} , and it might be related to the internal transition $\text{Cr}^{3+/2+}$ or to other deep traps present in LEC-grown crystals.⁸ Typically, such deep traps are present in concentrations in the range of 10^{14} – 10^{16} cm^{-3} . Such samples are also efficiently photosensitive⁴ in the near-infrared range. Under illumination the $I(V)$ characteristics are strongly dependent on temperature.

In the present work we report experimental results obtained by measuring the temperature dependence of the SNDC characteristics of Cr-doped GaAs samples for several illumination conditions. Our results show that the trap associated with SNDC characteristics lies about 90 meV below the minimum of the conduction band, instead of at the mid-gap internal transition $\text{Cr}^{2+/3+}$. We have shown that for our samples impact ionization occurs via electrons rather than via holes, despite the fact that the majority free carriers in the low-conductivity state are holes. The illumination discerns different LCS states because the free-carrier density varies, and we were able to study its influence on the impact ionization due to changes in the SNDC characteristics. The LCS is so strongly affected by illumination that it completely dominates the HCS at low temperatures.

EXPERIMENTAL DETAILS

In darkness and at room temperature Cr-doped GaAs samples are SI with carrier mobility around $4000 \text{ cm}^2 \text{ V}^{-1} \text{ s}^{-1}$. The samples were rectangular-bar shaped typically cut into 1.30-mm-width strips from a unique wafer. Two parallel indium contacts along the whole width were produced. The typical distance between the two contacts was $200 \mu\text{m}$. Contact diffusion was carried out at 300°C in a $\text{N}_2\text{-H}_2$ (85:15) reducing atmosphere for 25 min. The samples were placed on the cold finger of a gas-flux cryostat. For experiments carried out under illumination a GaAs infrared light-emitting diode (LED) was used as light source, and it was mounted near the sample inside the cryostat. Its energy emission has a peak at $E_g - 100 \text{ meV}$, where E_g is the energy gap of GaAs. The tunable photon flux for the geometry used

was assessed by $P \approx (2 \times 10^{10})I$ (photons/cm²s), where I is the current through the LED in milliamperes. This flux was calibrated by replacing the sample with a charge-coupled device. The electric current through the samples was obtained by measuring the voltage on a series resistor. Care was taken in order to avoid scale changes in the digital multimeters during the measurements, since this can lead to spurious ‘‘jumps’’ in the $\mathbf{j}(\mathbf{E})$ curves. We also prepared samples with the van der Pauw geometry in order to make Hall measurements.

RESULTS

On GaAs samples, most of the work found in the literature concerning SNDC characteristics was done at liquid-helium temperatures and for silicon-related shallow levels.^{9–13} In this case, free electrons in the conduction band (CB) and two electron levels due to silicon impurities are the basic requirements to explain the SNDC characteristic. Some work has been done on SI Cr-doped GaAs and SI GaAs with *EL2* centers.^{14–18} In both cases, most of the measurements were done at room temperature and illumination was not used. These measurements were mainly performed in structures of *p-i-n* diodes and the SNDC characteristic was observed in the $\mathbf{j}(\mathbf{E})$ curves at room temperature with a threshold electric field of a few kV cm⁻¹. Some authors claimed that the SNDC characteristics are due to impact ionization involving the mid-gap donor-acceptor deep traps, the CB, and the valence band (VB). The absence of systematic work reporting on the temperature and illumination dependencies was a motivation to carry out the measurements described in the present paper.

Hall measurements

In SI GaAs the Fermi level lies in the middle of the gap. Therefore, its electrical properties are close to those of the intrinsic materials. In fact, the Cr atom is an acceptorlike deep trap and the population of holes exceeds that of electrons. According to Look, Chaudhuri, and Eaves¹⁹ samples doped with Cr at 10¹⁷ cm⁻³ are SI at room temperature with Hall mobility around 4000 cm² V⁻¹ s⁻¹, and the ion concentrations are $[\text{Cr}^{2+}] = 7.8 \times 10^{16}$ cm⁻³, $[\text{Cr}^{3+}] = 5 \times 10^{16}$ cm⁻³, and $[\text{Cr}^{4+}] = 0$. The mobility value suggests that both free electrons and holes are involved in the transport properties. Since our sample is very similar to that of Look *et al.* we expect the ratio $[\text{Cr}^{2+}]/[\text{Cr}^{3+}] \approx 1.6$ to be roughly the same. Under this condition, Hall measurements are sensitive to both types of carriers and we must be careful with the interpretation of the Hall parameters. In Fig. 1 we show the temperature dependence of $\ln p$, where p is the Hall free-carrier density obtained in darkness. For our sample, the majority carriers are holes and the two activation energies were determined using Arrhenius fittings, namely, 0.75 and 0.13 eV for temperatures above and below 280 K, respectively. The 0.13 eV value is in good agreement with results of other authors and is associated with a lattice relaxation process of the deep traps of chromium atoms, resulting in a slower decay of free-carrier density for temperatures lower than 280 K.²⁰ The activation energy of 0.75 eV is the accepted value of the internal transition $\text{Cr}^{3+/2+}$, with holes being released in the

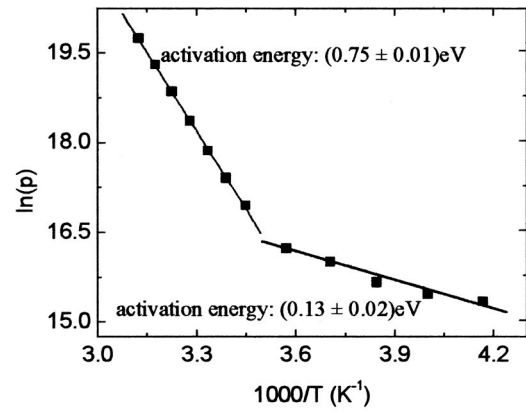


FIG. 1. Activation energies for in-darkness Hall measurements. Two activation energies were obtained: 0.75 ± 0.01 eV above 280 K and 0.13 ± 0.02 eV below 280 K.

valence band through the process $\text{Cr}^{3+} + \epsilon \rightleftharpoons \text{Cr}^{2+} + h$,¹⁹ where ϵ is the activation energy and h stands for the hole.

As shown in Fig. 2, at 290 K we have observed a monotonic increase of the electrical conductivity with the light intensity. The Hall effect measurements indicate that the electrical conductivity increases due to a major difference between the free hole and electron densities. This agrees with the results observed by other authors.⁵ They have shown that the ratio between the emission coefficients of holes and electrons is much greater than 1. Under illumination, with 10 mA in the infrared LED, the Arrhenius fit is poor. The Hall free-carrier density presents a superexponential behavior for decreasing temperature. This effect can probably be explained by the temperature dependence of the free-carrier lifetime due to different scattering mechanisms for each temperature region.

Temperature dependence of the resistivity and the SNDC characteristics in darkness

Our results are presented using the intensive variables \mathbf{j} and \mathbf{E} in order to eliminate the geometrical details of the sample. Despite the fact that the high-conductivity state has been previously associated with spatiotemporal structures,

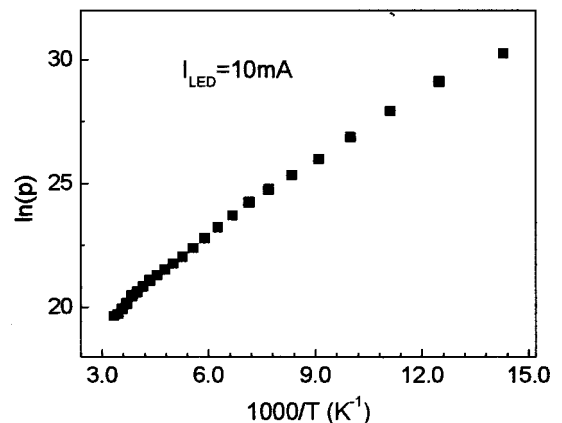


FIG. 2. Natural logarithm of Hall density under illumination as a function of the inverse temperature. The free-carrier density increases for decreasing temperature.

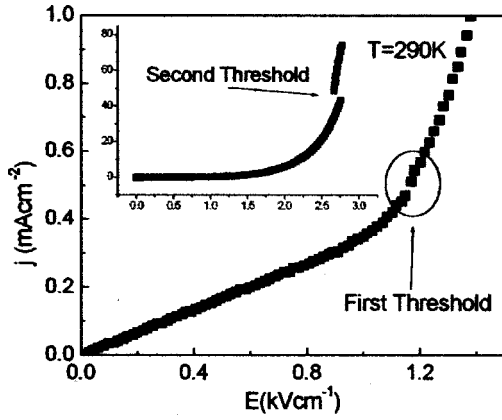


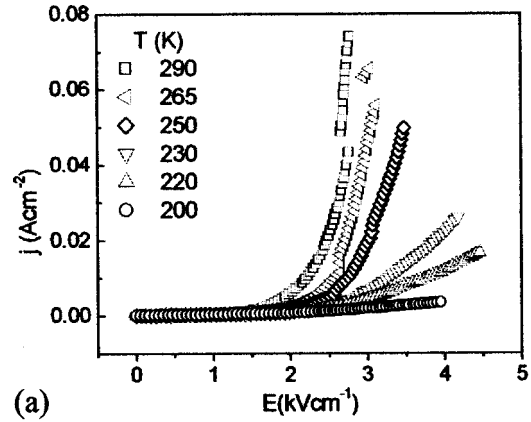
FIG. 3. In-darkness $j(E)$ characteristics for GaAs:Cr at 290 K. Two threshold electric fields can be identified around 1.1 and 2.7 kV cm^{-1} .

the j and E values for this case were obtained in the same manner as those for the low-conductivity state. The $j(E)$ characteristics obtained in darkness present an Ohmic regime in the LCS followed by a non-Ohmic HCS as shown in Fig. 3. At 290 K the Ohmic regime of the LCS dominates for electric fields up to about 0.9 kV cm^{-1} . At electric fields around 1.16 kV cm^{-1} occurs the first S-like instability, which cannot be easily seen in Fig. 3 due to the scale used. A second S-like instability is clearly observed, however, around 2.75 kV cm^{-1} .

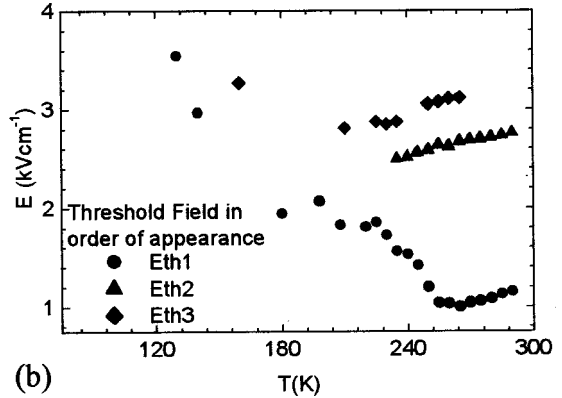
The temperature dependence of the $j(E)$ characteristics obtained in darkness is shown in Fig. 4(a). Three S-like instabilities were observed and their threshold fields are plotted as a function of temperature in Fig. 4(b). The differential resistivity $\rho_{\text{diff}} = (\partial j / \partial E)^{-1}$ of the HCS increases strongly on reducing the temperature. The range of the NDC region and its threshold electric field also depend on temperature. Figure 4(b) shows that the threshold electric field for the first instability E_{th1} decreases slowly down to around 260 K, where it starts to increase for further decrease in temperature. E_{th1} can be used as a rough indicator of the end of the Ohmic regime, i.e., the electric field reaches the value necessary for the onset of instability and the start of the HCS. The results presented in Fig. 4(a) were obtained by decreasing the temperature step by step after the measurement of each isothermal $j(E)$ characteristic. We have also carried out measurements by heating the sample to room temperature before its cooling to the new selected temperature. This was done in order to investigate the dynamic dependence of the S instabilities. Both procedures resulted in similar curves and for clarity only one of the methods is shown in Fig. 4(b).

The temperature dependence of the electrical resistivity for the LCS and HCS is shown in Fig. 5. For the LCS the electrical resistivity was directly obtained from the line slope and it presents a two-value function. It has a constant value in the temperature range between 290 and 220 K. Below 220 K the electrical resistivity presents a slightly higher value, i.e., it is about 10% higher. For the HCS, in contrast, the electrical resistivity should be obtained using the differential resistivity $\rho_{\text{diff}} = (\partial j / \partial E)^{-1}$ with j given by⁷

$$j = j_0 \exp(-\epsilon / e\lambda E), \quad (1)$$



(a)



(b)

FIG. 4. (a) In-darkness $j(E)$ characteristics for GaAs:Cr at different temperatures. (b) Temperature dependence of the threshold electric fields for three S-like instabilities.

where j_0 is the current density at the low-electric-field limit, ϵ is the trap energy, e is the electron charge, and λ is the mean free path determined by $\lambda = v_d \tau$, where v_d is the drift velocity. However, some ranges of the HCS can be fitted quite well into a linear approximation, giving a reasonable assessment for the differential resistivity. In this approximation, below 220 K, the resistivity increases monotonically and reaches the resistivity value of the LCS. Its variation ranges from $4 \text{ k}\Omega \text{ cm}$ at room temperature to $3000 \text{ k}\Omega \text{ cm}$ at 100 K. Moreover, the HCS and the electrical breakdown start to vanish for temperatures below 220 K.

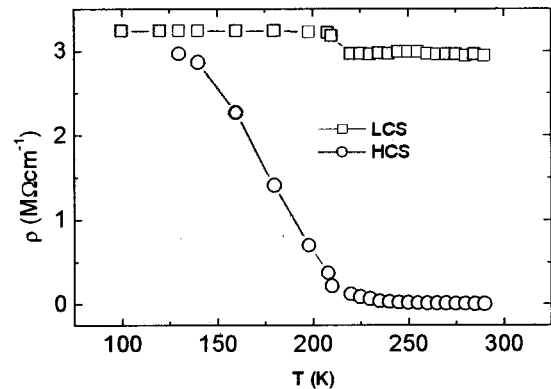


FIG. 5. Sample resistivity for the LCS and HCS in darkness as a function of temperature. At low temperatures the two regimes coalesce.

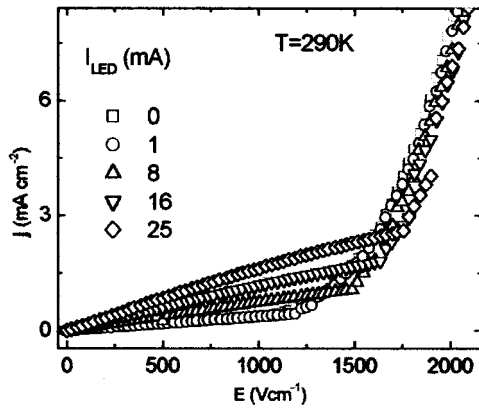


FIG. 6. $j(E)$ characteristics for GaAs:Cr at 290 K as a function of the illumination intensity. The threshold electric field increases with increasing illumination intensity.

Results under illumination

We have also carried out experiments under illumination. The sample was cooled in darkness to 290, 250, 225, 200, 175, 125, 100, and 85 K. The $j(E)$ characteristics were taken at each temperature in darkness and under different illuminations using the GaAs LED. To trace each set of isothermal measurements, the sample temperature was raised to 300 K after every measurement and then cooled down again. The results obtained at 290 K are shown in Fig. 6. The slope of the LCS increases with light intensity. This means that the sample became less resistive due to an increase in the free-hole density, as was found by the Hall measurements. The electric field range of the LCS increases with the light intensity, resulting in the crossing of the curves obtained under illumination with that obtained in darkness. The increase of the threshold electric field with the free-hole density indicates that the HCS occurs due to impact ionization by electrons. In the case of a HCS produced by impact ionization by holes the threshold field should decrease with increasing hole density.⁷

Although the linear fitting used in Fig. 5 is good enough to characterize the LCS over its whole range for darkness conditions, the linear dependence is lost under illumination. Indeed, even for results obtained at 290 K a slight downward bending, i.e., a sublinearity, is observed under illumination for LCS (see Fig. 6). The sublinearity is clearer for decreasing temperatures and increasing light intensities. The relationship changes so drastically that under high light intensity at 175 K, an NNDC in the $j(E)$ characteristic is even observed, as shown in Fig. 7. Only the typical effect of the in-darkness Ohmic regime remains at low temperatures. At intermediary temperatures however, the observed sublinearity and the high-conductivity regime coexist. Finally, it should be noted that the first part of the LCS in the $j(E)$ characteristics stays linear even under illumination and, as already pointed out, its slope increases substantially with increasing light intensity and decreasing temperature, as can be seen, e.g., in Fig. 7.

Another noteworthy feature is the tendency of the above-mentioned curve crossing to disappear for decreasing temperature. Indeed, at 250 K the curve crossing occurs only for

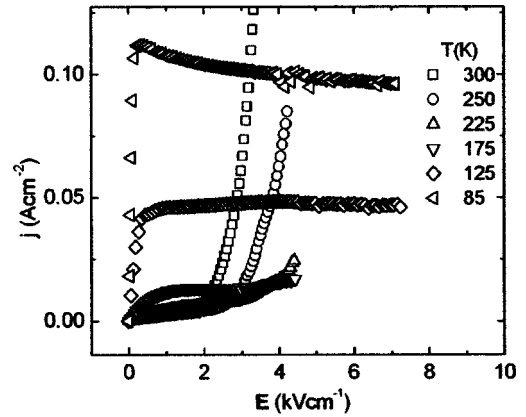


FIG. 7. $j(E)$ characteristics for GaAs:Cr with $I_{LED} = 30$ mA as a function of the temperature. There is an increasing field-enhanced trapping effect for decreasing temperature.

currents in the LED up to 10 mA. Higher current values do not produce crossing. In addition the S range is reduced for increasing illumination intensity. Indeed, although at 200 K the S instability is clearly observed in darkness, as can be seen in Fig. 8, it is hardly observed even for 0.1 mA in the LED.

DISCUSSION

SNDC characteristics

There is a controversy about the identification of the deep traps that are involved with the S instabilities in SI GaAs. The threshold field around 1 kV cm^{-1} that we have observed is too low to be associated with a mid-gap deep trap. Other authors found threshold electric fields ranging from 2 to 7 kV cm^{-1} .^{15,21} Paracchini and Dallacasa,²¹ using SI GaAs grown by the LEC technique in a silica crucible but without Cr, found an activation energy of 160 meV for the deep trap involved in impact ionization. They suggested that *EL10* or *EL11* centers, which are present in LEC-grown GaAs samples in smaller concentrations than the deeper *EL2* and *EL6* centers, are related to the S-like instability. Applying the same procedure as Paracchini and Dallacasa,²¹ we found an activation energy of 90 meV for the in-darkness measurements carried out at 290 K, assuming the mean free path λ as a constant in Eq. (1). We argue that this deep level is an

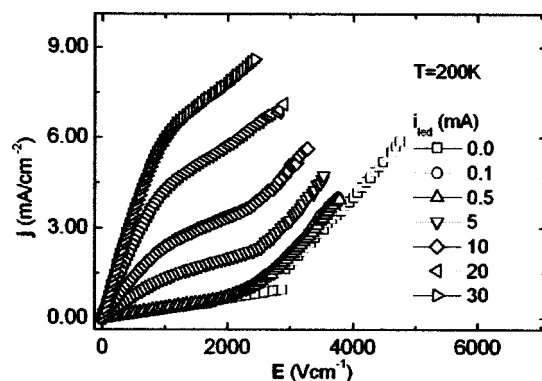


FIG. 8. $j(E)$ characteristics for GaAs:Cr at 200 K as a function of the illumination intensity. The threshold field disappears even under faint illumination.

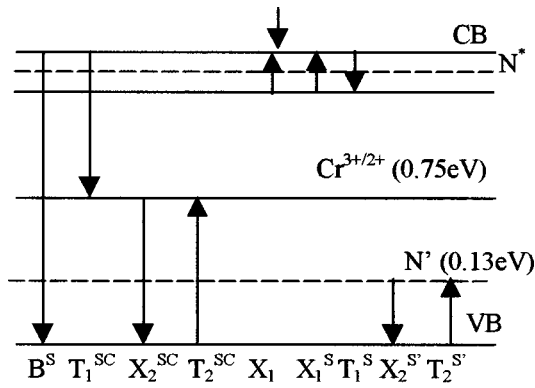


FIG. 9. Energy diagram for instabilities associated with one deep trap and two bands. B^S , T_1^{SC} , X_2^{SC} , T_2^{SC} , X_1 , X_1^S , T_1^S , X_2^S , T_2^S stands, respectively, for band-to-band recombination, CB-to-Cr electron capture, Cr-to-VB hole emission, VB-to-Cr hole capture, impact ionization for the 90 meV electron trap, 90 meV-to-CB trapped-electron emission, CB-to-90 meV electron capture, 0.13 eV-to-VB trapped-hole emission, and VB-to-0.13 eV hole capture.

electron trap rather than a hole trap, as schematically represented in Fig. 9. We propose that we are observing impact ionization induced by electrons. The reason for this proposal will be presented thoroughly below. In short, the dependence of the threshold electric field on the free-carrier density is the signature for the nature of the impact ionization. Using the temperature dependence of the in-darkness measurements, we also found that the intrinsic defect concentration involved in impact ionization is $1.4 \times 10^{16} \text{ cm}^{-3}$ with an ionization cross section of $1.3 \times 10^{-11} \text{ cm}^{-2}$. This last value suggests the presence of Coulombic scattering. Symanczyk,¹⁵ studying a Cr-doped SI GaAs p - i - n diode structure, found a threshold field around 7 kV cm^{-1} . This author suggests that the mid-gap level of Cr is involved in the S-like instability. In summary, the impurity level related to instabilities in SI GaAs involves intrinsic defects that appear during the growth of the crystals and seems to be different for different samples.

Having identified the 90 meV energy level, one question becomes relevant, namely, the role of the Cr atoms. We argue that the Cr level is not taking part in impact ionization but it is its presence that creates the conditions for the electrical breakdown involving the 90 meV electron trap. This trap is only poorly populated. Thus, to observe the S-like instability we need to keep the free-electron density at a very low level so that the electrons released into the conduction band by impact ionization can be multiplied efficiently enough to be experimentally detected. The role of the Cr atoms is then to keep the free-electron density at low values.

At thermodynamic equilibrium the Fermi level is pinned around a mid-gap position (at the Cr level) and the sample is highly compensated. The free-carrier density is extremely low, resulting in the SI characteristic of the sample. Under an external applied voltage, in order to generate the $\mathbf{j}(\mathbf{E})$ characteristic, the injected carriers are captured into the Cr level. This is true at least in the linear regime, since essentially the extra carriers injected in either of the two electrodes are trapped into the Cr level before they arrive at the other electrode. The effect of the applied electric field is to disturb the

thermodynamic equilibrium, producing a steady state, since the occupation of the Cr level depends on the value of the electric field. Quasi-Fermi levels, which are defined by the external applied voltage and by the temperature, must therefore be taken into account due to the relative population of the deep traps. The external electric field determines the injection efficiency and the temperature determines the trapping efficiency of the injected carriers. The SI characteristic of the sample remains, at least as long as the injected carriers are being captured in the deep traps. When a deep level is filled, another one, shallower than the previous one, starts to be filled. Following this process, the energy position of the trap being populated defines the quasi-Fermi level. The SI characteristic of the sample is undisturbed since neither the thermal energy nor the electric field succeeded in ionizing the deep traps. Nevertheless, when the injection process pins the quasi-Fermi levels in energy levels that are ionizable by impact, electrical breakdown is observed in the $\mathbf{j}(\mathbf{E})$ characteristics. Therefore the electronic injection is the mechanism that populates the 90 meV trap and impact ionization is the mechanism that causes its depopulation. Below the threshold electric field the injected electrons are trapped in the 90 meV trap since the recombination rate exceeds the impact ionization rate. For increasing electric fields the threshold electric field is achieved (it is characterized by the avalanche-like inversion of the recombination/ionization rate), and the HCS in the $\mathbf{j}(\mathbf{E})$ characteristic is observed. The Cr atoms create conditions for the observation of the breakdown (the avalanche process) involving the 90 meV electron trap, since it is the Cr level and eventually other deep traps that maintain the SI characteristic of the sample even at high temperatures.

Temperature and light-intensity dependence of the threshold electric field

As shown in Fig. 4(b), the value of the threshold electric field in darkness exhibits a slight decrease for temperatures decreasing from room temperature to about 260 K and a substantial increase for further temperature reduction. This observation must be related to the known fact that the threshold electric field increases for decreasing free-carrier density⁷—see also Eq. (3) below. Below 260 K, the increase of threshold electric field for decreasing temperatures is explained based on the reduction of the free-electron density following Boltzmann statistics for the 90 meV electron trap. On the other hand, the temperature dependence above 260 K cannot be explained based on the 90 meV electron trap. However, Hall measurements have indicated that below about 280 K the transport properties are defined by hole traps at an energy of 0.13 eV. Above 280 K the mid-gap level of the internal transition $\text{Cr}^{2+/3+}$, which interacts with both CB and VB, is the one that defines the transport properties. In this case, the Cr level controls the carrier densities in both the CB and VB due to a strong reduction in its free-carrier lifetime by many orders of magnitude when compared with those of the low-temperature regime. Hence, electrons released from the 90 meV electron trap are promptly captured in the Cr levels. Observe that this does not conflict with the assumption that the Cr is relevant only at low temperatures, as argued previously. Indeed, at low temperatures, field-enhanced trapping was claimed to be responsible for the enhancement of T_1^S (see Fig. 9). Therefore, at the high-

temperature limit, one observes a reduction in the free-electron density for increasing temperatures because the occupation ratio between the 90 meV energy level and the Cr level is reduced. This increases the threshold field, as observed for temperatures increasing from 260 to 290 K.

Theoretically, the dependence of the threshold electric field on the free-carrier density can be obtained from the rate equations using a simple model for one deep level and electrons in the CB, which yields the following expression:⁷

$$dn/dt = n[X_1 N_D^* - T_1^S(N_t - N_D^*) - n(X_1 + T_1^S)], \quad (2)$$

where N_t is the total deep-trap concentration, N_D^* the effective donor concentration, i.e., $N_D - N_A$, and the other parameters were defined in Fig. 9. The two steady states are obtained by setting $dn/dt = 0$. The first is $n_1 = 0$ and the second ($n_2 > 0$) occurs for

$$X_1 \geq X_{1c} = (N_t/N_D^* - 1)T_1^S. \quad (3)$$

The effect of illumination is to increase N_D^* , so that the critical impact ionization coefficient is reduced, providing in turn a reduction in the threshold electric field. Since the current density is essentially determined by the impact ionization coefficient X_1 —which has the same form as the current density [see Eq. (1)], namely, $X_1 = X_{10} \exp(-\varepsilon/e\lambda E)$ —a critical coefficient generates a threshold field in the $\mathbf{j}(\mathbf{E})$ characteristics. Therefore, the n -type minority carrier density in the LCS becomes the majority carrier density in the HCS. This rules out a threshold switching effect⁷ in our measurements, since the 90 meV electron trap cannot efficiently interact with both CB and VB.

The LCS in the Ohmic regime extends up to 1 kV cm^{-1} in darkness at 290 K and presents a sublinear behavior in the upper half when observed under illumination. This is more easily noticeable at low temperatures. This effect is the signature of field-enhanced trapping.²² The reduction of the free-hole density due to field-enhanced trapping must then be added to the reduction associated with the hole capture coefficient T_2^S for the reversed internal transition $\text{Cr}^{2+/3+}(\text{Cr}^{3+} + h\nu \rightleftharpoons \text{Cr}^{2+} + h\nu_{\text{VB}})$. In the temperature range³ from 150 to 400 K the dependence of T_2^S is given by $T_2^S = (1 \times 10^{-10})T^{0.5} \exp(-0.020/kT) \text{ cm}^3 \text{ s}^{-1}$. In our results, carried out in the range from 150 to 300 K, T_2^S follows this expression fairly well for low electric fields. The hole recombination mechanism associated with T_2^S due to the Cr level is the dominant effect. On the other hand, for high electric fields, field-enhanced trapping dominates for temperatures below 260 K, as observed experimentally. This explains why, for a constant light intensity, the threshold electric field inverts its tendency and reduces its value for decreasing temperatures [see Fig. 4(b)]. This effect is due to a reduction in the hole density and, consequently, a relative increase in the free-electron density.

In order to explain the presence of multiple S's—up to three S instabilities for the voltage range investigated—we consider two alternatives: multifilamentation or impact ionization of multiple deep traps. The multifilamentation phenomenon is characterized by the formation of adjacent current filaments; the current filament with the most favorable conditions survives and drains the other ones (“winner takes all”).²³ This kind of process is identified in the $\mathbf{j}(\mathbf{E})$ charac-

teristics by the formation of multiple S regions with the following constraint. The S at higher \mathbf{j} value has an electric field range larger than the previous one and includes the range of the previous one. On the other hand, multiple S's associated with multiple traps present S instabilities that do not have any correlation with the value of the electric field where they occur as is the case in multifilamentation. In our results, the three S instabilities do not fit the already mentioned condition and the S instabilities might be caused by at least two different traps. The second and the third S instabilities are vertically positioned, above each other and it might be that they are causing multifilamentation. The energy value of the second deep trap cannot be determined using the same procedure used to determine the 90 meV level, because of the overlap of impact ionization of the 90 meV level with that of the deeper one.

SUMMARY

We have studied the temperature and illumination dependence of the $\mathbf{j}(\mathbf{E})$ characteristic for a Cr-doped GaAs sample grown by the LEC method. We argue that the impurity levels related to instabilities in such samples involve defects appearing during the growth of the crystals and that are different for different samples. For our sample an electron trap with an energy level of 90 meV is related to the S instability observed at around 1 kV cm^{-1} . The neutral states of such impurities are kept low by the Cr atoms, and electron injection continuously moves the quasi-Fermi level until it aligns with the impurity level in order to finally produce the electrical breakdown. At least a second impurity is related to a second S-like instability observed at higher values of the external electric field. This second impurity level is fully occupied during the process of quasi-Fermi-level tuning by electron injection, so that the onset of the second electrical breakdown is tuned at a higher value of the electric field. Such results are supported by experiments started in different steady states, so that their influence on several physical features of the sample was easily observed. In this approach, the nonlinear behavior can be studied in a single sample for a broad range of initial conditions set up by the illumination. In particular, the great sensitivity of the S-shaped negative differential conductivity feature to the experimental parameters makes it an ideal physical system to be studied in the context of nonlinear physics. The dependence of impact ionization on the illumination was inferred from the SNDC characteristics. The low-conductivity state is strongly influenced by illumination. Based on the results obtained by varying the light intensity, we have shown that the trap with activation energy of 90 meV is an electron trap. Thus, electrons define the high-conductivity state and holes the LCS. As far as we know this is the first time that such an identification has been presented. By changing the temperature we were able to change the scattering mechanism, the carrier capture efficiency, and the optical emission efficiency of the traps involved.

ACKNOWLEDGMENTS

We would like to acknowledge the Brazilian agencies CNPq, FINEP, CAPES, and FAPEMIG for financial support.

- *Email address: rero@fisica.ufmg.br
- ¹J. B. Gunn, *Solid State Commun.* **1**, 88 (1963).
- ²S. M. Sze, *Physics of Semiconductor Devices* (Wiley, New York, 1981).
- ³J. S. Blakemore, *J. Appl. Phys.* **53**, 520 (1982).
- ⁴B. Clerjaud, *J. Phys. C* **18**, 3615 (1985).
- ⁵G. M. Martin, J. P. Farges, G. Jacob, J. P. Hallais, and G. Poiblaud, *J. Appl. Phys.* **51**, 2840 (1981).
- ⁶P. W. Green, *Semicond. Sci. Technol.* **13**, 116 (1998).
- ⁷E. Schöll, *Nonequilibrium Phase Transitions in Semiconductors* (Springer-Verlag, Berlin, 1987).
- ⁸R. M. Rubinger, J. C. Bezerra, E. F. Chagas, J. C. González, W. N. Rodrigues, G. M. Ribeiro, M. V. B. Moreira, and A. G. de Oliveira, *J. Appl. Phys.* **84**, 3764 (1998).
- ⁹A. Wacker and E. Schöll, *Z. Phys. B* **93**, 431 (1994).
- ¹⁰M. Gaa, R. E. Kunz, and E. Schöll, *Phys. Rev. B* **53**, 15 971 (1996).
- ¹¹W. Eberle, J. Hirschinger, U. Margull, W. Prettl, V. Novak, and H. Kostial, *Appl. Phys. Lett.* **68**, 3329 (1996).
- ¹²K. Kunihiro, M. Gaa, and E. Schöll, *Phys. Rev. B* **55**, 2207 (1997).
- ¹³K. Aoki and S. Fukui, *J. Phys. Soc. Jpn.* **67**, 1106 (1998).
- ¹⁴H. Rajbenbach, J. M. Verdiell, and J. P. Huignard, *Appl. Phys. Lett.* **53**, 541 (1988).
- ¹⁵R. Symanczyk, in *Nonlinear Dynamics and Pattern Formation in Semiconductors and Devices*, edited by F.-J. Niedernostheide (Springer-Verlag, Berlin, 1995), p. 200.
- ¹⁶H. C. Ellin, A. G. Jenpsen, and L. Solymar, *Appl. Phys. Lett.* **65**, 353 (1994).
- ¹⁷M. J. C. Manificier and R. Ardebili, *J. Appl. Phys.* **77**, 3174 (1995).
- ¹⁸J. Allam, R. Adams, M. A. Pate, and J. S. Roberts, *Appl. Phys. Lett.* **67**, 3304 (1995).
- ¹⁹D. C. Look, S. Chaudhuri, and L. Eaves, *Phys. Rev. Lett.* **49**, 1728 (1982).
- ²⁰B. K. Ridley, *J. Phys. C* **15**, 6865 (1982).
- ²¹C. Paracchini and V. Dallacasa, *Solid State Commun.* **69**, 49 (1989).
- ²²F. Piazza, P. C. M. Christianen, and J. C. Maan, *Appl. Phys. Lett.* **69**, 1909 (1996).
- ²³E. Schöll, *Braz. J. Phys.* **29**, 627 (1999).